Effect of substrate composition and topography on the improvement of wettability of titanium dioxide thin films

V. N. CANCEA[*a], V. ION[b], M. FILIPESCU[b], F. STOKKER-CHEREGI[b], M. DUMITRU[b], D. COLCEAG[b], M. D. IONITA[b], M. DINESCU[a,b]
[a]*Department of Physics, University of Craiova, 13 Al. I. Cuza Str., Craiova, 200585, Romania*
[b]*National Institute for Lasers, Plasma and Radiation Physics, P.O. Box MG 16, Magurele-Bucharest, 077125, Romania*

Abstract Titanium dioxide (TiO_2) thin films with specifically modified chemical composition, topography, and improved hydrophilic performances issued from Pulsed Laser Deposition (PLD) and Matrix-Assisted Pulsed Laser Evaporation (MAPLE) methods are obtained. Two types of substrates, with different morphologies are used: Si(100) and respectively parylene (poly-*p*-xylylene, PPX)-coated Si(100). The structure and surface morphology of the resulting TiO_2 thin films by Atomic Force Microscopy (AFM), Spectroscopic Ellipsometry (SE), X-Ray Diffraction (XRD), and Secondary Ion Mass Spectroscopy (SIMS) as well as the effect of the substrate topography on the hydrophilic properties of the TiO_2 thin films are analyzed.

(Received May 25, 2014; accepted July 10, 2014)

Keywords: TiO_2 thin films, PLD, MAPLE, AFM, SE, XRD, SIMS, wettability

1. Introduction

Due to its convenient optical, chemical, and wettability properties, TiO_2 was proved to be a challenging nano-material, used in a broad range of applications, from specialized branches like microfluidics to environmental procedures such as drinking water treatment to everyday goods like topical sunscreens. Thin films composed of TiO_2 nanoparticles are in particular appealing for applications in environmental remediation, field emission, gas sensing, electrochromics, and energy conversion/storage devices (e.g., solar cells, batteries). This potential is enabled by the unique photo (electro)chemical and electronic properties and high surface-to-volume ratio associated with TiO_2 nanostructures, which increase the sensitivity and the selectivity of photocatalytic, sensing and photovoltaic processes [1-6]. At the nanoscale level, the thermodynamic stability of the TiO_2 phases is strongly influenced by the degree of crystallinity, size and shape of the concerned crystallites [7,8], as well as the specific conditions in which they are formed [9-11]. The photoinduced hydrophilic property of TiO_2 has aroused lots of research interest in recent years [12-14]. This unique character presents numerous applications, such as self-cleaning, anti-fogging surfaces [15], as well as microfluidics. Recently, microfluidic systems for bio-analysis and chemistry research have been widely used in many fields, such as clinical diagnostics, genetic analysis, drug delivery, food safety, and environmental detection [16-18]. Since microfluidics requires an increase in the wettability of surfaces, TiO_2 was proved to provide practical application in this field [19].

Among the various deposition methods of TiO_2 thin films, PLD and its derivation, MAPLE, are significantly appropriate since they allow the precise control of various parameters, treatments, and factors over the desired chemical and physical properties of the resulting films. In PLD the material is ablated from a solid target, which can yield a significant variation in the size and morphology of the deposited particles [20-24]. By contrast, MAPLE is a physical vapor deposition process [25-27], similar to conventional PLD, but with different target preparation, namely the material to be deposited is firstly dissolved in some solvent (matrix) in various concentrations and then frozen as a solid target. Ideally, only the solvent should absorb laser radiation and then consequently evaporate, the dissolved material being transported by the vapors and finally collected on the substrate, like in PLD. Both methods are in principle suitable for most substrates, from relatively thermally stable ones (glass, silicon) to polymer and other thermolabile substrates such as poly-*p*-xylylene (PPX or parylene) [28, 29] or from flat and rigid to rough and flexible supports. Nevertheless, while PLD is more appropriate for substrate temperatures ranging from room to around 600 ºC, the MAPLE technique can successfully be used at room temperature and below [30].

In view of these, here we analyze the following aspects: 1. Ability of TiO_2 thin films to adopt different types of substrate morphologies – flat for Si(100) and porous (or displaying hierarchical structures) for parylene-coated Si(100) obtained by plasma polymerization; 2. Adequate deposition of TiO_2 thin films with specific properties by PLD and respectively MAPLE on both Si(100) and parylene-coated Si(100) substrates; 3. Structure and surface morphology properties of the resulting TiO_2 thin films by AFM, SE, XRD, and SIMS investigations; 4. Effect of the substrate topography on the hydrophilic properties of the TiO_2 thin films by means of water contact angle measurements.

2. Experimental setup

TiO_2 thin films have been deposited via two methods – PLD and MAPLE, using two kinds of substrates: Si(100) and parylene-coated Si(100). PLD titania thin films were obtained from a ceramic TiO_2 target using two laser systems: ArF from Coherent (193 nm wavelength, 40 Hz repetition rate) and respectively Nd:YAG Surelite SL II-10 by Continuum Company (1064 nm, 5-7 ns, 10 Hz). Each laser beam was focused on the target through a spherical lens under an incidence angle of 45° [31-34] at a laser fluence of 3 J/cm^2. Each substrate was placed at a distance of 4 cm from the target, parallel to the target, being kept at room temperature (RT=21°C). All PLD experiments were performed in oxygen background at 0.01 mbar. MAPLE depositions required the preliminary target preparation by pouring a solution of 5 wt. % and respectively 10 wt. % TiO_2 dissolved in double distilled water into the copper target holder and then by freezing it via gradually adding liquid nitrogen. TiO_2 thin films have been deposited by MAPLE using an Nd:YAG laser (266 nm, 5-7 ns, 10 Hz) at a fluence of 0.8 J/cm^2. The system (target) was maintained frozen during the experiments by liquid nitrogen cooling and the substrate-target distance was kept at 3.5 cm. Each target was rotated with a motion feedthrough driven by a motor, the laser beam describing a ring onto the sample, and the focusing lens was slowly translated (without modifying the incidence angle) in order to dig evenly within the sample and ensure a uniform target evaporation. All MAPLE depositions were undertaken in vacuum. The experimental setup is summarized in Table 1.

Table 1 Experimental setup for growth of TiO_2 thin films.

Sample	Deposition method	Target	Collector	P (mbar)	d_{t-c} (cm)	N_{Pulse}	Φ_{laser} (J/cm^2)	λ (nm)
1	PLD	TiO_2	Si(100)	0.01 O_2	4	80,000	3	193
2	PLD	TiO_2	PPX/Si(100)	0.01 O_2	4	80,000	3	193
3	PLD	TiO_2	Si(100)	0.01 O_2	4	40,000	3	1064
4	PLD	TiO_2	PPX/Si(100)	0.01 O_2	4	40,000	3	1064
5	MAPLE	TiO_2 (10 wt. %)	Si(100)	vacuum	3.5	40,000	0.8	266
6	MAPLE	TiO_2 (10 wt. %)	PPX/Si(100)	vacuum	3.5	40,000	0.8	266
7	MAPLE	TiO_2 (5 wt. %)	Si(100)	vacuum	3.5	40,000	0.8	266
8	MAPLE	TiO_2 (5 wt. %)	PPX/Si(100)	vacuum	3.5	40,000	0.8	266

3. Results and discussion

3.1 Atomic Force Microscopy

AFM images contain topographic information (with nanoscale resolution), meaning that each point is assigned a specific elevation (height). For each image the height scale is translated into a color scale. The darkest areas correspond to lowest heights and the lightest areas to the highest heights. The colors of the resulting images follow from combining topographic information with specific slope shading effects. The AFM images have been obtained with an XE-100 Park Systems microscope providing maximum and minimum scanning areas of 50x50 μm^2 and respectively of 500x500 nm^2.

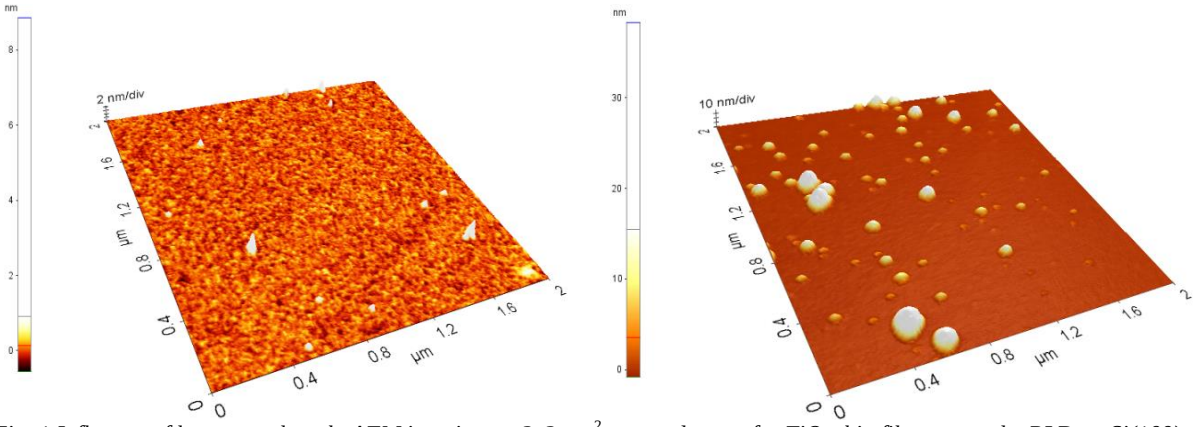

Fig. 1 Influence of laser wavelength. AFM imaging on 2x2 μm^2 scanned areas for TiO_2 thin films grown by PLD on Si(100) at 0.01 O_2 mbar: left – sample 1 (ArF –193nm, RMS 0.3 nm); right – sample 3 (Nd:YAG – 1064 nm, RMS 3.1 nm).

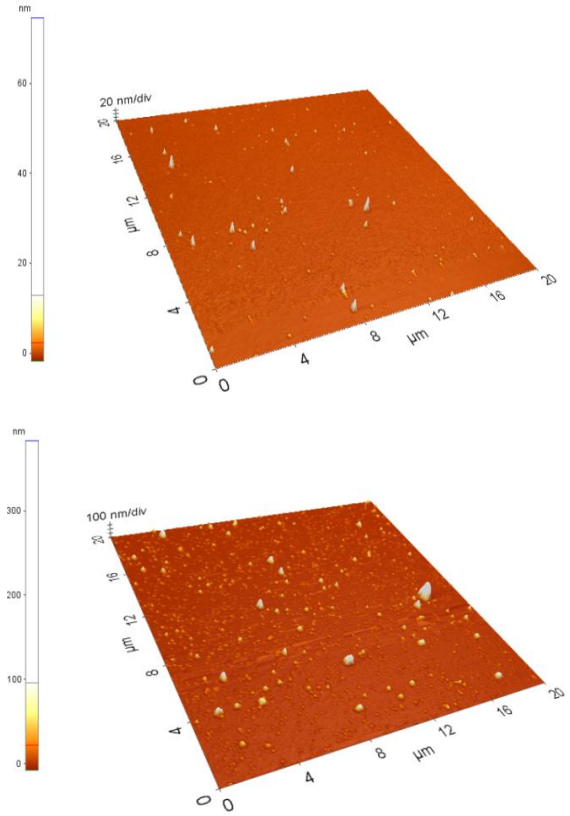

Fig. 2 Influence of laser wavelength. AFM imaging on 20x20 µm^2 scanned areas for TiO_2 thin films grown by PLD on Si(100) at 0.01 O_2 mbar: up – sample 1 (ArF – 193nm, RMS 1.5 nm); down – sample 3 (Nd:YAG – 1064 nm, RMS 12 nm).

Analyzing the influence of laser wavelength on the surface of TiO_2 thin films grown by PLD (Figs. 1 and 2), we observe that an increase in the wavelength from 193 to 1064 nm leads to an increase in the RMS (Root Mean Squared) roughness from 0.3 to 3.1 nm in relation to 2x2 µm^2 scanned areas and respectively from 1.5 to 12 nm with respect to 20x20 µm^2 scanned areas. Thin film surfaces issued from target irradiation with a 1064 nm laser beam present micrometric droplets and grains with sizes within 40-100 nm, while those obtained by target irradiation with a 193 nm beam are smooth, uniform, without pores or droplets.

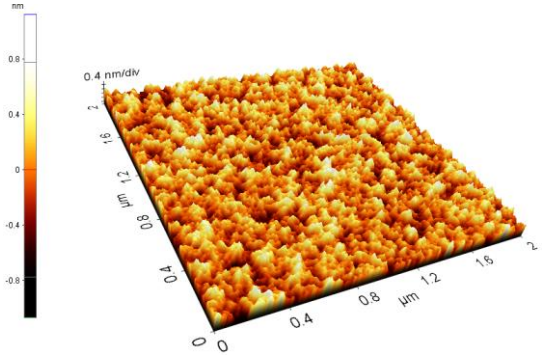

Fig. 3 AFM image of the parylene substrates deposited on Si(100), RMS: 0.3 nm.

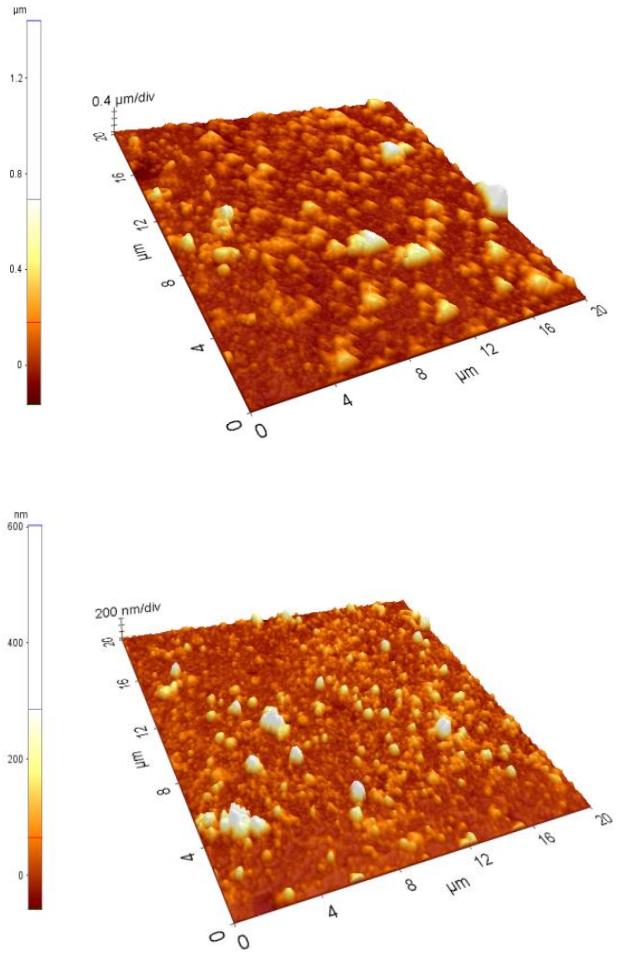

Fig. 4 Influence of TiO_2 concentration. AFM imaging on 20x20 µm^2 scanned areas for TiO_2 thin films grown by MAPLE on parylene in vacuum (Nd:YAG – 266 nm): up – sample 6 (10 wt.% TiO_2, RMS: 123 nm); down – sample 8 (5 wt.% TiO_2, RMS: 56 nm).

A set of TiO_2 thin films was grown by MAPLE in vacuum on parylene-coated Si(100) by irradiation with an Nd:YAG laser beam of 266 nm wavelength of targets prepared using aqueous TiO_2 powder solutions of different weight concentrations. The AFM investigation of the parylene substrate, prior to the deposition process, reveals a smooth surface, with a RMS roughness of 0.3 nm (Fig. 3), which therefore cannot influence the film growth. An increase in the TiO_2 concentration from 5 to 10 wt. % leads to an increase in the roughness from 56 to 123 nm for scanned areas of 20x20 µm^2 (Fig. 4), mainly due to a higher accumulation of grains from the target. The AFM analysis corresponding to 2x2 µm^2 scanned areas of TiO_2 thin films deposited on parylene-coated Si(100) (Fig. 5) shows that at a lower concentration (5 wt. %) the surface is being formed out of regular grains with sizes of approximately 50 nm. The same behavior is noticed for thin films grown also at different concentrations, but on Si(100) substrates.

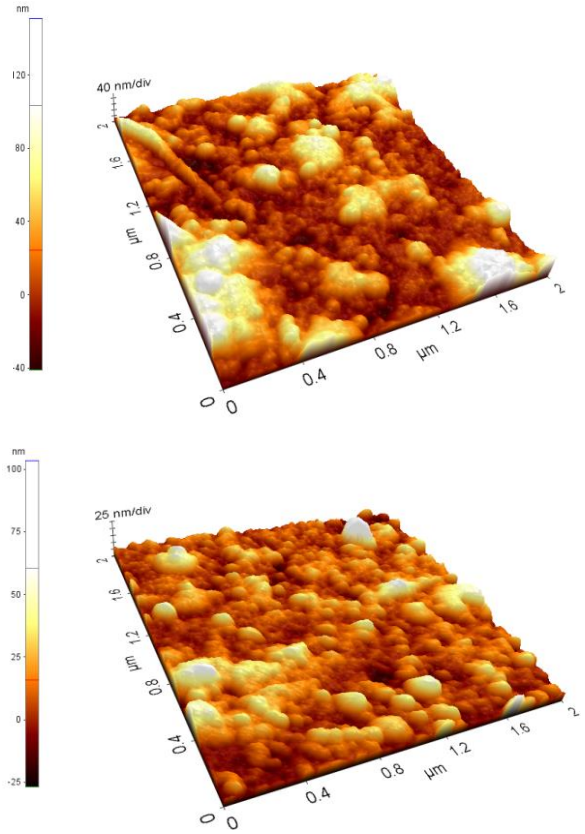

Fig. 5 Influence of TiO_2 concentration. AFM imaging on a 2x2 μm^2 scanned area for TiO_2 thin films grown by MAPLE on parylene in vacuum (Nd:YAG – 266 nm): up – sample 6 (10 wt.% TiO_2, RMS: 32 nm); down – sample 8 (5 wt.% TiO_2, RMS: 14 nm).

3.2 Spectroscopic Ellipsometry

Spectroscopic ellipsometry is a non-destructive experimental technique used to detect the change in the polarization of a light beam reflected or transmitted from a surface sample. The polarization change is represented as the change in amplitude ratio Ψ (Psi) and change in phase shift Δ (Delta), respectively between the p- and s-components of the light beam's electric field. Optical measurements have been performed with a Woollam Variable Angle Spectroscopic Ellipsometer (VASE) system equipped with a HS-190 monochromator.

Experimental data were acquired within a spectral range between 400 and 1000 nm, in steps of 2 nm, and at a beam incidence angle of 70°. The optical model used for fitting the experimental curves of the parameters Ψ and Δ is built from a sequence of four layers: the silicon substrate, a layer of native oxide of silicon of approximately 3 nm in thickness, the TiO_2 thin film deposited by either PLD or MAPLE, and a roughness layer taken as a Bruggemann approximation of equal material/air densities, 50% TiO_2 and 50% air (voids). The TiO_2 thin film was approximated as a Cauchy dispersion layer with Urbach absorption for MAPLE and respectively without absorption (transparent) for PLD.

The model is used to calculate the predicted response from Fresnel's equations (modeled curves for the parameters Ψ and Δ), which endows each material with thickness and optical constants. The calculated values are then compared to the experimental data. Finding the best match between the model and the experiment is typically achieved through regression. An estimator, like the Mean Squared Error (MSE), is used to quantify the difference between curves. The unknown parameters are allowed to vary until the minimum MSE is reached.

In Fig. 6 are given both the experimental and modeled curves of the parameters Ψ and Δ (the latter according to the previously mentioned optical model) as well as the values of the Cauchy and Urbach parameters resulting from the fitting process (see figure insets) for TiO_2 sample 7 on Si(100) deposited by MAPLE. The dependence of the refraction index *n* and respectively of the extinction coefficient *k* on wavelength by means of the above Cauchy and Urbach parameters are shown in Fig. 7. It can be seen that within the investigated spectral range this sample displays a rather large optical absorption (large extinction coefficient) and a refraction index smaller than that specific to TiO_2. Meanwhile, the thickness of the TiO_2 thin film for this sample is of approximately 40 nm with a matching roughness (around 46 nm). These results are conveniently explained under the hypothesis that the deposited TiO_2 layer is porous. The values of the refraction indices represent in fact an average between TiO_2 and air (voids) values of *n*.

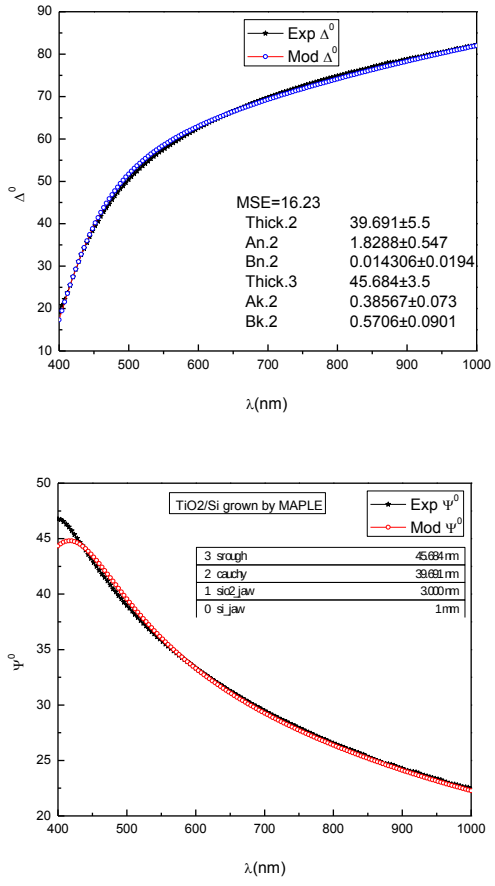

Fig. 6 Experimental and modeled curves of the parameters Δ and Ψ for TiO_2/Si sample 7 grown by MAPLE.

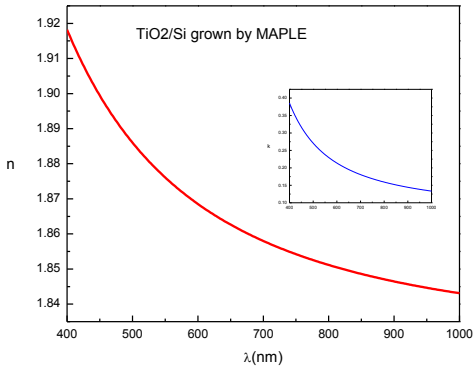

Fig. 7 The dependencies of n and k (inset) on wavelength for TiO_2/Si sample 7 grown by MAPLE.

Regarding the TiO_2 thin films deposited on the same substrate like before, Si(100), but by PLD, we use the same arguments regarding the acquisition and processing of experimental data up to the observation that we no longer need the assumption of Urbach absorption for building up the optical model. This is because we know from the literature that the values of the extinction coefficient are very small for a certain region within the spectral range (for instance 10^{-4} at 400 nm), where PLD TiO_2 thin films are practically transparent. Therefore, for this region only, it is enough to adopt an optical model simply subject to Cauchy dispersion.

In Fig. 8 are given the results of the fitting process (experimental and modeled) with respect to the TiO_2/Si sample 3, including the Cauchy parameters An and Bn in the inlet of the left-side figure. Consequently, Fig. 9 contains the graphic representations of the refraction index *n*: one generated from the previous fitting (red) and the other theoretical (black), known from the literature [35] for anatase TiO_2.

From the two figures below it can be concluded that the value of the thickness for the TiO_2/Si sample 3 is around 70 nm with a small roughness of about 1 nm, while the values of the refractive index are comparable with the results from the literature.

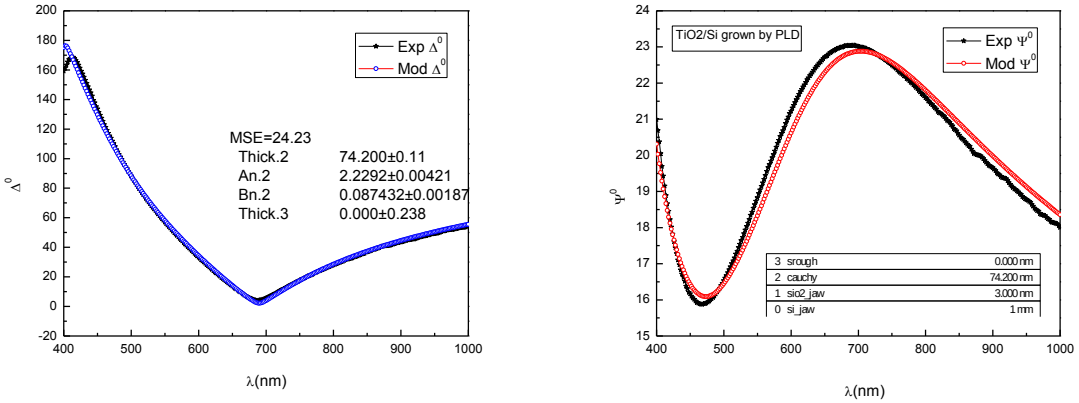

Fig. 8 Experimental and modeled curves of the parameters Δ and Ψ for TiO_2/Si sample 3 grown by PLD.

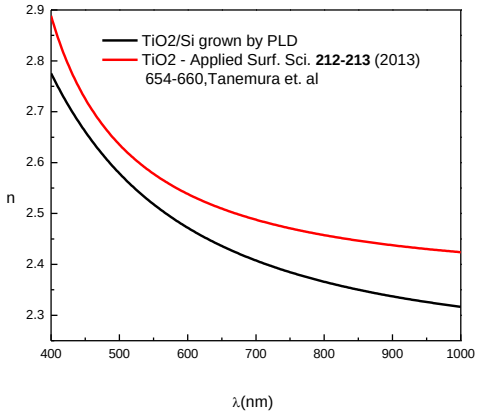

Fig. 9 The dependence of n on wavelength for TiO_2/Si sample 3 grown by PLD.

As a general conclusion of the spectroscopic ellipsometry analysis for TiO_2 thin films, we can state that from the perspective of film quality (smaller roughness, refraction indices in agreement with those known from the literature, etc.) the PLD method offers better results. The MAPLE deposition procedure generates rougher TiO_2 films, more porous, and thus with higher values of specific surface, being therefore more suitable for applications in medicine and biology.

3.3 X-Ray Diffraction

The XRD analysis of all thin film structures presented in this paper has been performed with a PANalytical's X'Pert PRO MRD (Materials Research Diffractometer) system with standard $\Theta - 2\Theta$ Bragg-Brentano diffraction geometry.

Thin films deposited by PLD are amorphous to XRD; meanwhile, samples obtained by MAPLE show a crystalline structure. The GI-XRD patterns of as deposited films in comparison with their corresponding substrates (parylene) reveal the formation of TiO_2-anatase phase only for a high TiO_2 concentration target.

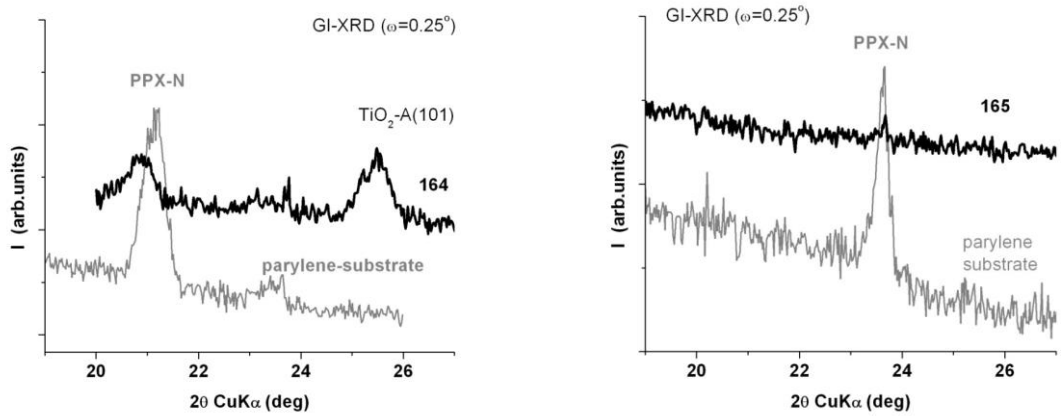

Fig. 10 XRD patterns for TiO_2 thin films grown by MAPLE on parylene in vacuum (Nd:YAG – 266 nm) at different concentrations: up – sample 6 (10 wt.% TiO_2);down – sample 8 (5 wt.% TiO_2).

3.4 Secondary ion mass spectroscopy

The equipment used for the investigation of compositional analysis of PLD-grown titania films is provided by Hiden Analytical. Primary ions are generated by an Ar^+ beam at an injection voltage of 5 kV, an intensity of 100 mA, and a pressure of 3×10^{-5} mbar.

The *depth profiling* records emphasize that the samples grown by PLD exhibit a relatively uniform distribution of elements (O, Ti) (Fig. 11), while those deposited by MAPLE show a clear imbalance among their in-depth components (Fig. 12), mainly due to their small thickness.

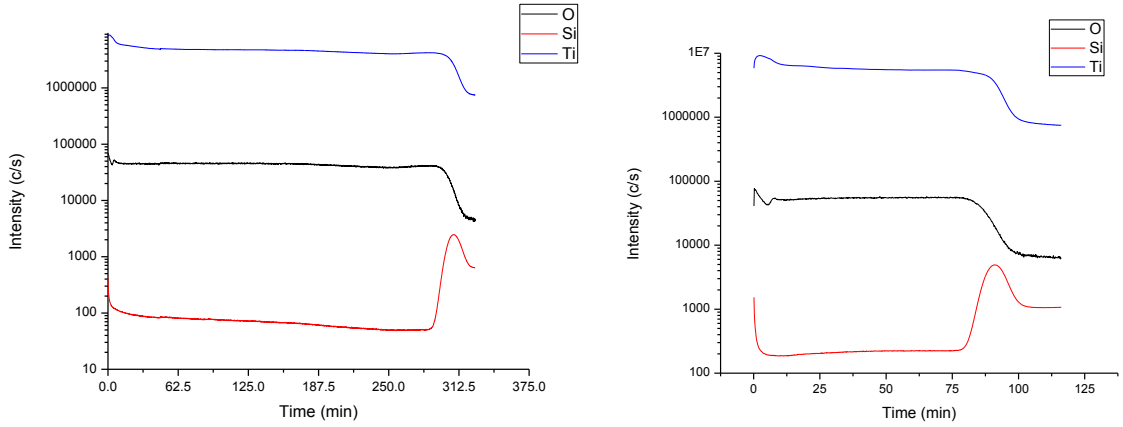

Fig. 11 Depth profile for TiO_2 thin films grown by PLD on Si(100) at different laser wavelengths:up – sample 1 (193 nm); down – sample 3 (1064 nm).

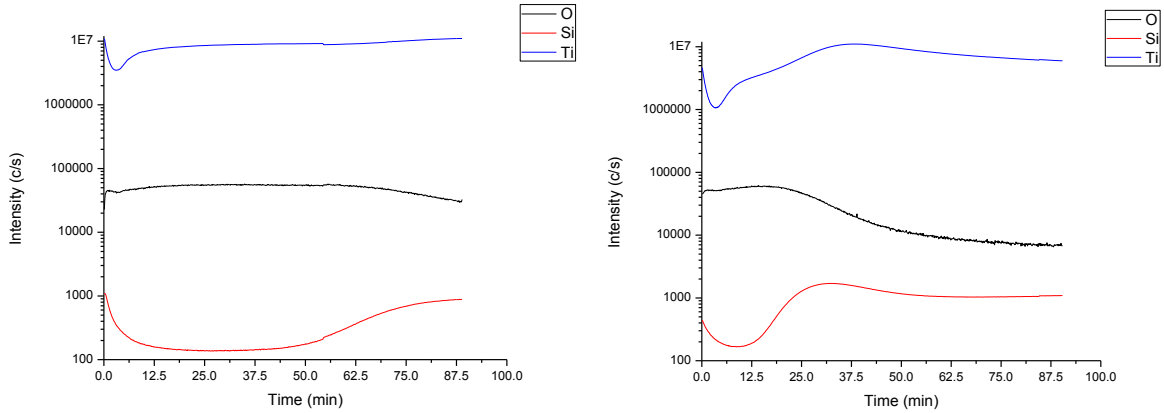

Fig. 12 Depth profile for TiO_2 thin films grown by MAPLE on parylene in vacuum (Nd:YAG – 266 nm) at different concentrations: up – sample 6 (10 wt.% TiO_2); down – sample 8 (5 wt.% TiO_2).

3.5 Mean Contact Angle

TiO_2 thin films grown by various methods are known to display appealing properties from the perspective of bio-medical applications [36-37]. Among these, preliminary in-vitro bio-compatibility tests like the study of cell attachment and cell proliferation [38] are strongly required. In order to perform such tests TiO_2 films are firstly probed for certain physical properties, among which the hydrophilic behavior [12-14] plays a special role due to the fact that hydrophilic surfaces seem to attract water out of the environment and thus facilitate the growth of cells or micro-organisms affixed to them.

Physically speaking, the hydrophilic or hydrophobic behavior of surfaces is related to wettability, which is analyzed via mean (water) contact angle measurements. Thus, if the mean contact angle is less than 90º the surface is considered hydrophilic, while for mean contact angles greater than 90º surfaces are hydrophobic (very small values of this angle, close to 0º, define super-hydrophilic layers, in contrast to very large values, close to 180º, which disclose super-hydrophobic areas). In the case of rough surfaces, like the TiO_2 thin films analyzed here, specialized devices are required in order to perform proper computations.

The mean contact angle measurements for all the TiO_2 samples listed in Table 1 have been done with a CAM 200 series Drop Profile Analysis Device from KSV Instruments Ltd. All the investigated TiO_2 samples display hydrophilic features, characterized by a minimum value of the mean contact angle of 43.13º with a standard deviation of 1.95º for sample 6 TiO_2/parylene, see Fig. 13, up to a maximum value of 80.18º for sample 7 TiO_2/Si with a standard deviation of 0.92º (Fig. 14).

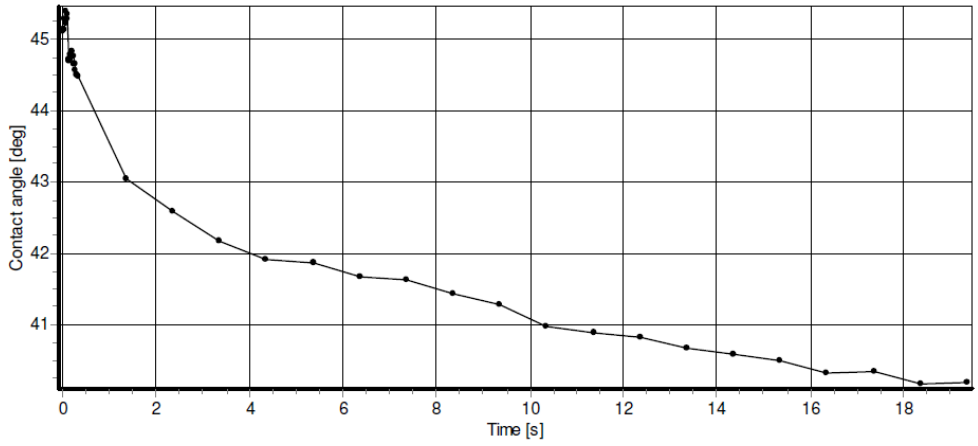

Fig. 13 Variation of the contact angle over time for sample 6 TiO_2/parylene.

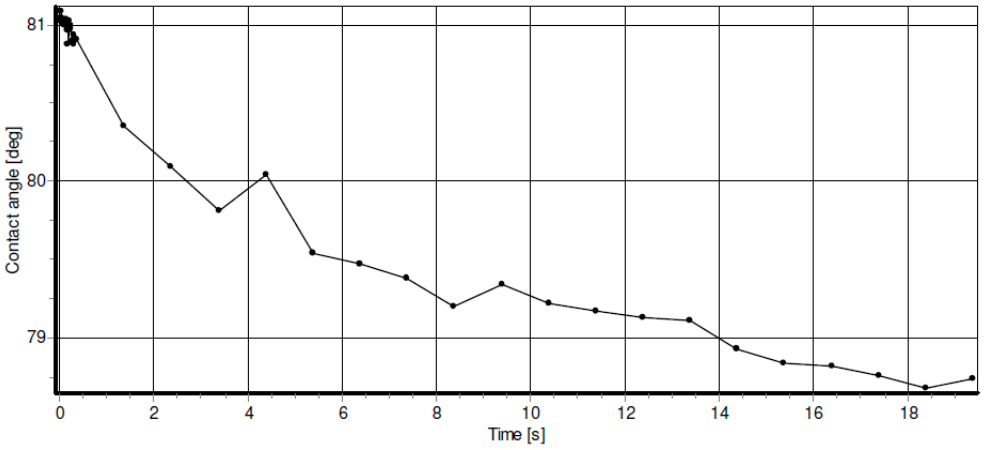

Fig. 14 of the contact angle over time for sample 7 TiO_2/Si.

Examining the CAM records of all TiO_2 thin films we observe that those deposited on parylene-coated Si(100) substrates display smaller values of the mean contact angle, which recommends them for further in-vitro bio-compatibility tests.

4. Conclusions

The PLD technique favors the formation of smooth and uniform TiO_2 thin films, without defects, and leads to an increase in the roughness with the laser wavelength, while the MAPLE deposition favors an increase in the

roughness with the increase of TiO_2 concentration (porous surfaces), irrespective of the substrate surface morphology (for parylene coatings). The layers are amorphous or poorly crystalline (TiO_2 anatase phase is identified by XRD). The layers prepared by PLD method exhibit very small extinction coefficients (are practically transparent), with values of the refractive index comparable with those from the literature, while those obtained by MAPLE are less transparent and with smaller values of the refractive index. The substrate topography affects the wettability properties of TiO_2 thin films: the presence of parylene over a silicon substrate leads to more hydrophilic surfaces.

Acknowledgement

One of the authors (V.N.C.) acknowledges support from the strategic grant POSDRU/159/1.5/S/133255, Project ID 133255 (2014), co-financed by the European Social Fund within the Sectorial Operational Program Human Resources Development 2007 – 2013.

References

[1] U. Bach, D. Lupo, P. Compte, J. E. Moser, F. Weissortel, J. Salbeck, H. Spreitzer, M. Gratzel, Nature **395**, 583 (1998).
[2] H. G. Yang, C. H. Sun, S. Z. Qiao, J. Zou, G. Liu, S. C. Smith, H. M. Cheng, G. Q. Lu, Nature **453**, 638 (2008).
[3] J. Jiu, S. Isoda, F. M. Wang, M. Adachi, J. Phys. Chem. B **110**, 2087 (2006).
[4] B. Liu, E. S. Aydil, J. Am. Chem. Soc. **131**, 3985 (2009).
[5] P. G. Su, C.-T. Lee, C. Y. Chou, K.-H. Cheng, Y. S. Chung, Sens. Actuators B-Chem. **139**, 488 (2009).
[6] H. Y. Jeong, D.-S. Lee, H. K. Choi, D. H. Lee, J.-E. Kim, J. Y. Lee, W. J. Lee, S. O. Kim, S.-Y. Choi, Appl. Phys. Lett. **96**, 213105 (2010).
[7] A. S. Bernard, L. A. Curtiss, Nano Lett. **5**, 1261 (2005).
[8] A. S. Bernard, P. Zapol, J. Phys. Chem. B **108**, 18435 (2004).
[9] M. P. Finnegan, H. Zhang, J. F. Banfield, J. Chem. Phys. C **111**, 1962 (2007).
[10] M. P. Finnegan, H. Zhang, J. F. Banfield, Chem. Mater. **20**, 3443 (2008).
[11] C. B. Mendive, T. Bredow, A. Feldhoff, M. A. Blesa, D. Bahnemann, Phys. Chem. Chem. Phys. **11**, 1794 (2009).
[12] R. Wang, K. Hashimoto, A. Fujishima, M. Chikuni, E. Kojima, A. Kitamura, M. Shimohigoshi, T. Watanabe, Nature **388**, 431 (1997).
[13] R. Wang, N. Sakai, A. Fujishima, T. Watanabe, K. J. Hashimoto, Phys. Chem. B **103**, 2188 (1999).
[14] D. H. Shin, T. Shokuhfar, C. K. Choi, S. Lee, C. Friedrich, Nanotechnology **22**, 315074 (2011).
[15] O. Carp, C. L. Huisman, A. Reller, Prog. Solid State Chem. **32**, 33 (2004).
[16] D. C. Duffy, J. C. McDonald, O. Schueller, G. M. Whitesides, Anal. Chem. **70**, 4974 (1998).
[17] A. Arora, G. Simone, G. B. Salieb-Beugelaar, J. T. Kim, A. Manz, Anal. Chem. **82**, 4830 (2010).
[18] P. Liu, R. A. Mathies, Trends Biotechnol. **27**, 572 (2009).
[19] N. Liu, H. Li, H. Wang, T. Chen, J. Wang, L. Chang, Matt. Lett. **89**, 247 (2012).
[20] J. W. Yoon, T. Sasaki, N. Koshizaki, Appl. Surf. Sci. **197–198**, 684 (2002).
[21] T. Sumita, T. Yamaki, S. Yamamoto, A. Miyashita, Appl. Surf. Sci. **200**, 21 (2002).
[22] T. Sumita, T. Yamaki, S. Yamamoto, A. Miyashita, Thin Solid Films **416**, 80 (2002).
[23] A. K. Sharma, R. K. Thareja, U. Wilier, W. Schade, Appl. Surf. Sci. **206**, 137 (2003).
[24] M. Zhu, T. Chikyow, P. Ahmet, T. Naruke, M. Murakami, Y. Matsumoto, H. Koinuma, Thin Solid Films **441**, 140 (2003).
[25] D. B. Chrisey, A. Pique, R. A. McGill, J. S. Horwitz, B. R. Ringeisen, D. M. Bubb, P. K. Wu, Chem. Rev. **103**, 553 (2003).
[26] J. Schou, Appl. Surf. Sci. **255**, 5191 (2009).
[27] A. Luches, A. P. Caricato, Appl. Phys. B **105**, 503 (2011).
[28] I. Y. Gotlib, D. V. Filyukov, S. W. de Leeuw, Polym. Sci. Ser. A **51**, 583 (2009).
[29] D. R. Strel'tsov, E. I. Grigor'ev, P. V. Dmitryakov, N. A. Erina, K. A. Mailyan, A. V. Pebalk, S. N. Chvalun, Polym. Sci. Ser. A **51**, 881 (2009).
[30] S. Acquaviva, M. Fernández, G. Leggieri, A. Luches, M. Martino, A. Perrone, Appl. Phys. A **69**, S471 (1999).
[31] R. Dinu, M. Dinescu, J. D. Pedarnig, R. A. Gunasekaran, D. Bäuerle, S. Bauer-Gogonea, S. Bauer, Appl. Phys. A **69**, 55 (1999).
[32] P. Verardi, M. Dinescu, F. Craciun, Appl. Surf. Sci. **154/155**, 514 (2000).
[33] F. Craciun, P. Verardi, D. Brodoceanu, M. Morar, C. Galassi, C. Grigoriu, M. Dinescu, Mater. Sci. Semicond. Proc. **5**, 227 (2002).
[34] I. Vrejoiu, D. G. Matei, M. Morar, G. Epurescu, A. Ferrari, M. Balucani, G. Lamedica, G. Dinescu, C. Grigoriu, M. Dinescu, Mater. Sci. Semicond. Proc. **5**, 253 (2002).
[35] S. Tanemura, L. Miao, P. Jin, K. Kaneko, A. Terai, N. Nabatova-Gabain, Appl. Surf. Sci. **212–213**, 654 (2003).
[36] H.-J. Oh, J.-H. Lee, Y.-J. Kim, S.-J. Suh, J.-H. Lee, C.-S. Chi, Mater. Chem. Phys. **109**, 10 (2008).
[37] M. Zuber, S. Tabasum, T. Jamil, M. Shahid, R. Hussain, K. S. Feras, K. P. Bhatti, J. Appl. Polym. Sci. **131**, DOI:10.1002/app.39806 (2014).
[38] M. Dinescu, A. Matei, V. Dinca, A. Palla-Papavlu, F. Di Pietrantonio, D. Cannata, M. Benetti, E. Verona, T. Lippert, Rom. Rept. Phys. **65**,1019 (2013).

* Corresponding author: virgil_ucv@yahoo.com